NATIONAL ADVISORY COMMITTEE FOR AERONAUTICS

TECHNICAL NOTE 2580

AN ANALYSIS OF AN X-RAY ABSORPTION METHOD FOR MEASUREMENT OF HIGH GAS TEMPERATURES

By Ruth N. Weltmann and Perry W. Kuhns

Lewis Flight Propulsion Laboratory
Cleveland, Ohio

Washington
December 1951

NATIONAL ADVISORY COMMITTEE FOR AERONAUTICS

TECHNICAL NOTE 2580

AN ANALYSIS OF AN X-RAY ABSORPTION METHOD FOR MEASUREMENT OF HIGH GAS TEMPERATURES

By Ruth N. Weltmann and Perry W. Kuhns

SUMMARY

An analysis is presented of an X-ray absorption method for determining high gas temperatures which can be applied over a wide range of temperatures. The indicated temperature represents the mean density of the gas. For known shapes of temperature profiles, any desired mean temperature can be calculated.

At high temperatures (above 1800° K for hydrocarbon combustion gases), dissociation affects the values of some of the parameters. For this reason a correction factor is defined and calculated as a function of temperature (up to 3000° K) for stoichiometric mixtures of hydrocarbons and air.

Design suggestions for a practical instrument of optimum sensitivity in temperature measurement are given on the basis of a theoretical analysis, which is corroborated by a few experimental data.

INTRODUCTION

Measurements of high gas temperatures are required in the evaluation of the performance of reaction propulsion equipment. The present upper limit of thermocouple use is approximately 2000° K, and probably this value cannot be extended much without serious loss in calibration stability. Other techniques for measuring high gas-temperatures are radiation methods, which depend either upon the spectral brightness of gaseous flame or upon the absorption of excited atoms such as salts added to the flame. Most of these methods are only applicable in a limited temperature range; where the temperature is nonuniform, the actual temperature evaluation is rather difficult even for known temperature profiles.

The X-ray absorption method of temperature measurement has an advantage over most optical radiation techniques because it is not limited to a small temperature range. The measurement is an indication of the gas density integrated over the path length and the temperature can be readily calculated from the density and static-pressure determinations for known shapes of temperature profiles. The calculation can be performed to yield various types of mean temperature.

A laboratory arrangement for applying X-ray absorption determinations to the measurement of the extremely high temperature of a direct-current nitrogen discharge arc is described in reference 1.

A theoretical analysis of the factors involved in the measurement of the temperature of gaseous combustion products by the X-ray absorption method is presented herein. Consideration is given to the corrections required for gaseous dissociation at extremely high temperatures, and dissociation and air-gas-mixture correction factors are calculated for stoichiometric mixtures of hydrocarbons and air. In addition, the errors introduced by the uncertainty in the temperature profiles are indicated.

Since the error in the measurement depends largely on the design of the instrument, structural details are considered and a design for a practical temperature X-ray absorption instrument is suggested. The relative error in temperature measurements is calculated for such an instrument when applied to a 1.5-foot path length, hot tunnel, test section. Different temperature operating conditions and design features are presented.

An experimental laboratory setup with a 4.25-inch burner was built and used to evaluate some of the suggested design features. The experimental X-ray absorption temperature data were used to corroborate part of the theoretical analysis.

THEORY

Absorption Equation

Measurement of the temperature of a gas by the X-ray absorption method is based on Lambert's law and the ideal gas law. When the gas law $\rho = \frac{PM}{R_g T}$ is introduced into the modified absorption equation $I = \frac{I_o AC}{d^2 4\pi} e^{-B\rho L}$, the following general relation is obtained:

$$I = \frac{I_o CA}{d^2 4\pi} \exp\left(-\frac{1}{R_g}\int_o^L \frac{BMP}{T}\,dL\right) \qquad (1)$$

where

I X-ray intensity after absorption

I_o initial X-ray intensity

C absorption factor, indicative of absorption before entering and after leaving test section

A cross-sectional area of X-ray beam at distance d from X-ray tube

d distance from X-ray source to detector

R_g universal gas constant

B mass-absorption coefficient of gas mixture in test section

M molecular weight of gas mixture

P gas pressure

T gas temperature

L path length through gas mixture

For convenience, all symbols in this report are defined in appendix A.

From equation (1), for constant temperature and pressure over the path length L,

$$T = \frac{PLMB}{R_g \ln (K/I)} \tag{2}$$

where $K = \frac{I_o CA}{4\pi d^2}$ and is constant for each experimental setup. The constants K and B can be obtained by calibration. In most cases, however, it seems advantageous to employ a reference intensity and to make an intensity-ratio measurement rather than to determine the absolute value of K. The value of B depends on the applied X-ray voltage if air is used, as shown in figure 1.

Two alternative reference methods are suggested: either the use of the X-ray intensity I_a through air at air density ρ_a corresponding to the reference pressure P_a and room temperature T_a or the application of a vacuum-reference intensity I_v.

The vacuum reference permits the use of the density corresponding to the measured temperature in determining the lowest voltage that can be applied. This technique has an advantage over the air-reference method where the lowest voltage is determined by room-temperature density. Substitution of F for MB/M_aB_a in equation (2) yields, for room-temperature air reference:

$$T = \frac{T_a F}{1 - \left[\frac{1}{B_a I \rho_a} \ln\left(\frac{I}{I_a}\right)\right]} \tag{3a}$$

and, for vacuum reference:

$$T = \frac{B_a \rho_a T_a F}{\ln\left(\frac{I_v}{I}\right)} \tag{3b}$$

For both equations (3) and throughout the following analysis, the pressure of the gas being measured is assumed to remain constant and equal to the reference pressure. If the pressure of the gas being measured differs from the pressure of the reference gas, the factor F, wherever it occurs in the temperature equation, must be multiplied by the ratio of the pressures.

Evaluation of F

In equations (3), if no dissociation occurs, F is independent of temperature and is designated as F_u; in the presence of dissociation, F varies with temperature. Where the temperature of the gas mixture is unknown, the temperature may be first calculated as if no dissociation occurred by using F_u in equation (3). If dissociation is expected, (dissociation of the products of combustion of hydrocarbons and air starts at a temperature of about 1800° K), the calculated temperature is multiplied by a dissociation factor F/F_u and the actual temperature is obtained by successive approximation. In figure 2, F is plotted as a function of temperature for stoichiometric mixtures of the series of saturated hydrocarbons with air. For the calculation of F, use is made of reference 2.

The different values of F are calculated from the equation

$$F = \frac{\sum_i M_i m_i \sum_j k_j p_j}{\left(\sum_i M_i m_i \sum_j k_j p_j\right)_a} \tag{4a}$$

which, for any air-reference method, reduces to

$$F = \frac{\sum_i M_i m_i \sum_j k_j p_j}{28.93} \tag{4b}$$

where m and p are the molecular and atomic percentages per unit volume of gas, and k is the atomic emission coefficient, approximately proportional to the fourth power of the atomic number A, such that $k \approx 1.6 \times 10^{-4} A^4$. The quantity $\sum_j k_j p_j$ for air is approximately equal to 1. The atomic emission coefficients of some elements are given in table I. For calculation of F for nonstoichiometric mixtures, use may be made of reference 3.

Evaluation of Errors

The relative error in temperature measurement $\Delta T/T$ is given by

$$\left[\frac{\Delta T}{T}\left(1 - \frac{T}{F}\frac{\partial F}{\partial T}\right)\right]^2 = \left[\frac{T}{T_a}\frac{1}{B_a \rho_a L F}\frac{\Delta I}{I}\right]^2 + \left[\frac{\Delta F}{F}\right]_F^2 \qquad (5)$$

where $\Delta I/I$ is the relative error in intensity measurement, $(T/F)(\partial F/\partial T)$ is the fractional uncertainty in F for a given relative error in the temperature (obtainable from fig. 2 for saturated hydrocarbons in stoichiometric mixture with air), and $(\Delta F/F)_F$ is the uncertainty in F due to uncertainty in knowledge of the gas constituents and of the dissociation products. If no dissociation is present, $F = F_u$ and $\partial F/\partial T = 0$. Since the quantity $\partial F/\partial T$ is always negative, the presence of known dissociation decreases the error in temperature determination.

According to equation (5), the error in temperature measurement depends on the error $\Delta I/I$ of intensity measurement and on the product $B_a I \rho_a$. When a Geiger-Mueller counter is employed as X-ray detector, the relative probable error in counting is, by statistical theory,

$$\frac{\Delta I}{I} = 0.67 \frac{\sqrt{N + N_B}}{N - N_B} \qquad (6)$$

where N is the total count and N_B the background count. In most practical cases, a relative error of $\Delta I/I = \pm 0.03$ is found for a $B\rho L$ of about 2 at room-temperature air-reference conditions and of about 5 at vacuum-reference conditions if a 1- to 2-minute measuring time for a counting rate of about 500 to 1000 counts per minute is used. For these counting times and rates, and if F is assumed to be about 1, the relative error in temperature measurement is approximately $\pm 0.015 \frac{T}{T_a}$ and $\pm 0.006 \frac{T}{T_a}$, for the room-temperature air- and vacuum-reference methods, respectively.

Nonuniform Temperature Distribution

In equations (3) the temperature is assumed constant over the path length L. If the temperature varies along the path, the indicated temperature is equal to $\left(\frac{1}{L}\int_0^L \frac{1}{T}\,dL\right)^{-1}$ and is thus proportional to the mean density $\bar{\rho}$ since $\bar{\rho} = \frac{PMT_a\rho_a}{P_aM_aL}\int_0^L \frac{1}{T}\,dL$. The relative error in density is the same as the relative error in temperature given by equation (5).

An important measurement application occurs when the shape of the temperature distribution is known or can be estimated, but the absolute values of the temperature are unknown. The ratio of local temperature to some reference temperature, expressed as a function of path length, will be termed the "temperature profile." If pressure is assumed constant over the path length, the temperature at any point can be calculated from the measured X-ray intensity and from one measured temperature such as T_a. An appropriate integration of the temperature profile inside the test section will in turn relate the temperature at any point to a desired mean temperature.

A passage, the temperature profile of which is symmetrical with respect to the center of the passage, will be considered as an example and the errors introduced by uncertainty as to the shape of the temperature profile will be evaluated. For convenience, the temperature profiles will be represented by power functions. For the profile inside the test section, the following relation will be assumed:

$$T_r = \frac{T_c}{1 + \alpha\left(\frac{r}{R}\right)^n} \quad \text{for} \quad r \leq R \tag{7}$$

where

T_r temperature along the radial distance

T_c temperature at path center

α $\frac{T_c - T_w}{T_w}$

T_w wall temperature

r radial distance

R one-half measured path length, $2R = L$

n inside profile exponent

For $\frac{r}{R} < 1$, $\lim_{n \to \infty} T_r = T_c$ and the temperature over the path length approaches a constant value as n increases.

In practical cases, when the X-ray source and detector cannot be mounted directly on the test section, the X-rays will traverse two outside path lengths $\frac{d-L}{2}$ in addition to the path length L of the test section. In order to minimize absorption effects on the measurements, the density along part of the outside path should be kept constant and low by evacuation. The portion of the outside path that is adjacent to a hot test section may exhibit a density gradient through its unevacuated length D because of the existence of a temperature gradient. The outside profile along the length D, if assumed to be a power function and symmetrical with respect to the center line of the test section, can be expressed as

$$T_r = \frac{T_w}{\beta \left(\frac{r-R}{D} \right)^q + 1} \quad \text{for} \quad R \leq |r| \leq (R+D) \tag{8}$$

where

β $\frac{T_w - T_a}{T_a}$

n outside profile exponent

For a constant outside profile, $\lim_{q \to \infty} T_r = T_w$ for $\frac{r-R}{D} < 1$, and $\lim_{q \to 0} T_r = T_a$ for $\frac{r-R}{D} > 0$. Examples of inside and outside profiles which follow equations (7) and (8) are shown in figure 3. In the following analysis, T_w, n, and q are assumed to be independent constants. (A problem in which T_w and q are functions of T_c is treated in appendix B.)

Substituting equations (7) and (8) in equation (1), integrating, and assuming M, B, and P constant over the path length give

$$T_c = \frac{T_a \left(\frac{n}{n+1} \right) F}{1 - \frac{1}{2B_a \rho_a R} \ln \left(\frac{I}{I_a} \right) - \frac{T_a}{T_w} \left(\frac{F}{n+1} \right) + \frac{D}{R} \left(\frac{q}{q+1} \right) \left(1 - \frac{T_a}{T_w} \right)} \tag{9a}$$

if room-temperature air-reference intensity is used or

$$T_c = \frac{T_a \left(\frac{n}{n+1}\right) F}{\frac{1}{2B_a\rho_a R} \ln\left(\frac{I_v}{I}\right) - \frac{T_a}{T_w}\left(\frac{F}{n+1}\right) - \frac{D}{R}\left(\frac{q}{q+1}\right)\left(\frac{1}{q} + \frac{T_a}{T_w}\right)} \tag{9b}$$

if a vacuum-reference intensity is used. In equations (9), F is assumed equal to 1 throughout the path length D.

For regions where dissociation does not occur, F in equations (9) is replaced by F_u. When dissociation is present and the value of F is uncertain because of its variation with temperature, the temperature, corrected for dissociation, can be computed by successive approximation by use of the recursion formula

$$T_c = (T_c)_9 \frac{F}{F_u}\left[\frac{1}{1 + \frac{T_c}{T_w n}\left(\frac{F_u - F}{F_u}\right)}\right] \approx (T_c)_9 \frac{F}{F_u}\left[1 - \frac{(T_c)_9}{T_w n}\left(\frac{F_u - F}{F_u}\right)\right] \tag{10}$$

where $(T_c)_9$ is the value computed from equation (9) for successive approximations of F. In the temperature range where $\frac{(T_c)_9}{T_w n}\left(\frac{F_u - F}{F_u}\right) \leq 0.01$ this term can be neglected and $T_c \approx \frac{F}{F_u}(T_c)_9$. The expression for the relative error in temperature measurement is similar in form to equation (5) except for the addition of factors representing the uncertainty in knowledge of the inside and outside profiles. The complete expression then becomes:

$$\left[\frac{\Delta T}{T}\left(1 - \frac{T}{F}\frac{\partial F}{\partial T}\right)\right]^2 = \left[\frac{T_c}{T_a}\left(\frac{n+1}{n}\right)\frac{1}{2B_a\rho_a RF}\frac{\Delta I}{I}\right]^2 + \left[\frac{\Delta F}{F}\right]_F^2 + \left[\left(\frac{\frac{T_c}{T_w} - 1}{\frac{T_c}{T_w} + n}\right)\left(\frac{\Delta n}{n+1}\right)\right]^2 + \left[\frac{D}{FR}\left(\frac{T_c}{T_a} - \frac{T_c}{T_w}\right)\left(\frac{n+1}{n}\right)\frac{\Delta q}{(q+1)^2}\right]^2 \tag{11}$$

If no dissociation is present, so that F is independent of temperature, $F = F_u$ and $\partial F/\partial T = 0$. In the presence of dissociation, the same considerations apply as for equation (5).

2401

Neglect of the outside profile, corresponding to omission of the final term in equation (9), is equivalent to introduction of a fractional temperature error

$$\frac{D\left(\frac{T_c}{T_a} - \frac{T_c}{T_w}\right)\left(\frac{q}{q+1}\right)}{RF\left(\frac{n}{n+1}\right)}$$

For $D \ll R$, this error becomes negligible. The fractional temperature error obtained when the inside profile is neglected is approximately

$$\frac{\frac{T_c}{T_w} - 1}{\frac{T_c}{T_w} + n}$$

which becomes negligible only as $T_c \to T_w$ or as $n \to \infty$. Hence, in most applications the inside profile must be considered carefully in the temperature calculations, if accurate results are required.

METHOD OF APPLICATION

Instrumental Considerations

In order to apply the X-ray absorption method to the measurement of flame and gas temperatures, a setup similar to that shown schematically in figure 4(a) is used. Commercial X-ray generating equipment can be employed in conjunction with an X-ray tube provided with a beryllium window since low X-ray accelerating voltages (below 10 kv) are required in most cases. The X-rays pass from the X-ray tube through an evacuated chamber, a minimum air space of length D, the test flame-gas path of length 2R, another air space of length D, and an evacuated chamber to a Geiger-Mueller counter. The counter is suitably connected to a commercial scaler to allow the counting of pulses and thus to give the intensity reading. The flame can be either open or, if enclosed, surrounded by a casing provided with portholes to permit the undisturbed passage of the X-ray beam. The cooled ends of the evacuated chambers on each side of the burner are closed off by thin aluminum foil windows or by a series of three or more portholes along the direction of the X-ray beam, as shown in figure 4(b). At high temperatures, a gas of low X-ray absorption, such as helium, can be used to cool the windows and to reduce the effective absorption of the space between the windows and the burner. The Geiger-Mueller counter should be provided with thermal-radiation shielding and cooling since it should be kept at about 300° K.

In an X-ray absorption instrument, the error in the temperature measurement depends on certain mechanical features and the various X-ray beam parameters. This error relation is given in equation (5) for a constant temperature profile and in equation (11) for varying inside and outside temperature profiles. Both equations indicate that it is desirable to combine a low counting error $\Delta I/I$ with a high mass-absorption coefficient B. Since the counting error decreases with increasing X-ray accelerating voltage (reference 4), whereas the absorption coefficient B decreases with increasing voltage (fig. 1), a compromise is required to yield optimum sensitivity.

Mechanical Features

As shown by equation (1), for a constant applied voltage and a fixed burner condition, the intensity increases with the size of detector area A and with the absorption factor C, which decreases with the amount of absorption in the length (d-2R) and also decreases with the total X-ray path length d. The absorption factor C should be made to approach unity as closely as possible, which is achieved in the design by making the total path length d such that (d-2R) is as small as mechanically feasible and by evacuating as much of the length (d-2R) as possible. The absorptions through the air spaces D and through the windows must still be considered. The only advantage in using windows instead of pinholes is that a large detecting area A, may be obtained on the receiver side. While the opening diameter with windows may be made as large as 0.20 inch without serious danger of window breakage, the largest diameter of the pinholes should not exceed about 0.05 inch. Thus the detecting area for windows may be 16 times that for pinholes. On the other hand, aluminum windows must be cooled below 1000° K and thus require an air space D of at least 1 inch, whereas a recess of about 0.25 inch from the burner may suffice for the pinhole arrangement. The use of a smaller air space D decreases the absorption and reduces the error introduced by lack of information on the exact shape of the outside profile, as can be seen from equation (11). The order of magnitude of the absorption factor C for two different window conditions is obtainable from figure 5 by determining the ratio of the ordinates of one of the curves to the ordinates of the curve for no windows.

The portholes in the burner should be made at least as large as the detector area to permit free passage of the X-ray beam, and should allow for the effects of thermal expansion.

X-Ray Beam Parameters

The selection of the X-ray parameters should be such as to give the smallest error in temperature measurement. As indicated in equation (5) and in the discussion of that equation, the highest mass-absorption coefficient B should be combined with a sufficiently large count to give a small counting error. A large number of counts can, of course, always be obtained by counting over longer periods of time. The duration of the measurement, however, is frequently limited when dynamic conditions prevail. For unlimited counting time, the counting error approaches zero even for a low counting-rate intensity, provided that the measured count is larger than the background count.

In order to obtain a working curve suitable for determination of the proper X-ray tube operating voltage for a desired intensity, the following experiment was performed at a given accelerating voltage: Distance L or D was varied to produce an intensity of 1000 counts per minute with a Machlett X-ray tube, Type A-2 Diffraction Tube, with a tungsten target at a 15-milliampere filament current. The value of L or D and the value of B from figure 1 were inserted in the expression $\frac{A}{d^2} e^{-B\rho L}$. This expression is plotted in figure 5 as a function of accelerating voltage. The ordinates of this curve may be taken to represent $\frac{1000}{N_c} \frac{A}{d^2} e^{-B\rho L}$, where N_c is the number of counts per minute in any experiment. When known or desired values of A, d, L, ρ, B, and N_c are inserted in the expression for the ordinates and figure 1 is used to relate B to the accelerating voltage, a plot can be made on figure 5 that will intersect the three curves shown on the figure. The intersection of this plot with the curve of desired window condition yields the X-ray voltage required to give an intensity of N_c counts per minute. The parameters L, d, and A are inherent in the design; ρ is the maximum density that will be encountered in the contemplated experiment and corresponds either to the room-temperature air-reference if a room-temperature air-reference method is employed or to the lowest test temperature if a vacuum reference is used. The vacuum reference is preferred for higher sensitivity in high-temperature measurements because its use permits employment of lower X-ray voltages and thus attainment of higher mass-absorption coefficients. The counting accuracy may be calculated from equation (6) and the expected error in temperature measurement from equation (5). A desired low error in temperature measurement can be obtained in a minimum counting time by properly adjusting the counting rate and mass absorption coefficient.

When temperature profiles are present, the manner of selecting the X-ray parameters is still valid, but the relative error in the temperature measurement is then calculated from equation (11) and depends largely on the ratio D/R and on the uncertainty of knowledge of the temperature profiles.

Computations for 1.5-Foot Path Length Section

In figure 6 are shown the relative errors in temperature measurement as calculated from equation (5) for a 1.5-foot path length, hot tunnel, test section of flat profile and optimum construction for various design and operating temperatures. Design temperature is that gas temperature for which the apparatus is designed to give highest sensitivity; operating temperature is the actual temperature in the test section. The gas is assumed to be a product of the stoichiometric combustion of saturated hydrocarbons with air, and dissociation corrections have been applied in accordance with figure 2. Some of the calculations have been made for both reference methods. The error curves in figure 6(a) clearly indicate the advantage of the vacuum-reference method, especially for measurements in the higher temperature ranges. Figure 6(b) indicates the decrease in error obtained by decreasing the time of measurement while maintaining a constant total count. In order to obtain the approximate error in temperature measurement for any other desired total count, the values given in figure 6(b) may be multiplied by the square root of the ratio of counting times. The advantage of using aluminum foil windows instead of pinholes wherever temperature conditions permit is indicated in figure 6(c). At the lower counting rates, windows are less advantageous because of the larger absorption of the softer X-rays by the window material. All curves in figure 6 indicate that decrease in the error in temperature measurement is obtained in the temperature range in which dissociation occurs and when accurately known corrections for dissociation have been applied.

The intensity ratio I/I_v for constant parameters of wall and center temperatures, X-ray path length, X-ray beam conditions, and gas mixture, are shown in figure 7 as a function of the exponents n and q (equations (7) and (8)). In most practical cases, q will lie between 1 and 2 and n will lie between 3 and 15, so that a 10-percent change in I/I_v would be produced by a change from $n = 3$ to $n = 15$. The sensitivity function $(\Delta I/I)/\Delta T$ at $T = T_c$ is equal to $\frac{2B_a\rho_a RFT_a}{T_c^2}\left(\frac{n}{n+1}\right)$ (equation (11)) and is independent of q. The sensitivity function is plotted in figure 8 for the same constant parameters as those used in figure 7. From this plot it is seen that the X-ray intensity must be measurable within 4 percent if $n = \infty$ (flat profile) and within 3 percent if $n = 3$, in order to measure the center temperature of 1800° K to within 100° K. The sensitivity varies inversely as the square of the center temperature. Hence, in order to measure a temperature of 900° K within 50° K, the X-ray intensity has to be obtained within 6 percent if $n = 3$.

EXPERIMENTAL INVESTIGATION

Apparatus and Procedure

Photographs of the experimental setup appear in figure 9. This setup was designed to achieve simplicity of construction rather than to obtain optimum sensitivity of temperature measurement. The outside unevacuated path length D is large compared with the path length L being measured, so that a large error is introduced if the density profile along D is not accurately known. In addition, a room-temperature air-reference method was used, so that the results (as shown in fig. 6) were less favorable than they might have been if a vacuum-reference method had been used. The primary purpose of the experiments was to establish design data. The experimental data, in addition, were used to corroborate the theoretical considerations which led to equation 9(a).

The burner consisted of a cast-iron pipe 4.25 inches in diameter and 18 inches in length. An Inconel burner plate with 22 holes each of 0.3-inch diameter was the top surface of the mixing chamber which was 22 inches long. The holes were arranged in three rows parallel to each other and to the direction of the X-ray beam, so that the flame filled the diameter of the pipe at the line of X-ray beam passage. Portholes for the path of the X-ray beam were provided in the burner pipe at positions 8.5 and 13.5 inches above the burner plate. The portholes were 0.5 inch in diameter to assure free passage of the X-ray beam even in the presence of possible misalinement due to thermal expansion and vibration.

The X-rays generated in a Machlett, Type A-2 Diffraction Tube, passed through an evacuated chamber of 5.1-inches length, an 0.0035-inch aluminum foil window, the burner pipe, and a second aluminum foil window to a Geiger-Mueller counter. In order to prevent overheating of the Geiger-Mueller tube window, a radiation shield 0.5-inch deep with a 0.25-inch diameter porthole was used. Cooling coils were employed at each aluminum foil window, which was separated by about 1.0 inch of air space from the burner pipe. The Geiger-Mueller counter was connected to a commercial scaler from which the X-ray intensities were read.

Because on ignition of the flame a positive pressure tended to collapse the aluminum foil windows, especially when a vacuum existed at the other side of the window, evacuation of the connecting chambers was postponed until after ignition. The height and the temperature of the flame were varied by changing the fuel-air mixture. At the lower portholes, a center temperature range from 1630° to 1700° K was obtainable, whereas the center temperature at the upper portholes could be varied from 1390° to 1510° K after steady-state conditions had been reached.

A platinum - 87-percent platinum plus 13-percent rhodium bare-wire thermocouple was used for the comparison temperature measurements. All thermocouple indications were corrected for radiation losses (reference 5). For each X-ray absorption temperature determination, thermocouple temperature measurements were made inside the gas-flame mixture at seven points distributed along the 4.25-inch diameter of the burner pipe to obtain the inside profile, and at the 0.5-inch point of the 1.0-inch air space to obtain the outside profile. In addition, the wall temperatures of the burner pipe were determined at the portholes. The average reference temperature (room temperature) for all experiments was 300° K.

The selected accelerating X-ray voltage of 4.15 kilovolts resulted in a counting rate of about 600 counts per minute at room temperature and in a higher counting rate at higher temperatures.

Results

Typical inside and outside profiles for the experimental burner are plotted in figure 10 for three determinations at a measured center temperature of about 1510° K. The continuous curves in figure 10 are the profiles calculated from equations (7) and (8) for $n = 4$ and $n = 8$ for the inside burner, for a center temperature equal to the measured center temperature of 1510° K, and for an average $T_w/T_{D/2}$ of 2.1 for the outside air space, corresponding to $q = 1.2$.

The measured and corrected thermocouple temperatures and the experimental X-ray absorption intensity data are tabulated in table II. In addition the X-ray intensity ratios calculated from equation (9a) are listed for the radiation-corrected thermocouple temperatures and for an average inside profile exponent $n = 6$. Comparison of the experimental and theoretical intensity ratios yields a mean error of ±4 percent and the mean deviation of the experimental intensity ratio values is ±6 percent. The experimental error includes a statistical standard deviation of ±2 percent, and the remaining deviation may be caused partly by temperature-time fluctuations but is more likely caused by lack of precision in operational technique. An X-ray voltage shift of 0.1 kilovolt would account for more than 5-percent change in intensity ratio. By exercising care and by employing additional indicating meters, the X-ray voltage could have been readily adjusted to within 0.01 kilovolt.

The wall temperature T_w as well as the outside profile exponent q tended to increase with increasing center temperature T_c as shown in table II. Most of the T_w and q values obtained at the upper burner portholes can be approximated by linear functions of T_c. The solid

line in figure 11 represents theoretical intensity ratios calculated from equation (9a) by using the T_w and q functions, as shown in appendix B. In addition, the experimentally obtained X-ray absorption intensity ratios are plotted in figure 11 against the radiation-corrected thermocouple center temperatures. The agreement between the experimental points and the theoretical curve indicates the possibility of using the X-ray absorption method to measure high gas temperatures and verifies the validity of equation (9a) in the presence of temperature profiles. From the equation in appendix B, the error in temperature measurement appears to be of the order of the experimental error in X-ray intensity ratio measurement. Evaluation of the X-ray temperatures by graphical interpolation from figure 11 yields a mean error of ±4 percent (table II), which is about the same as the mean error in intensity ratio measurement.

CONCLUDING REMARKS

Theoretical analysis indicates that X-ray absorption measurements are applicable to the measurement of high temperatures of combustion gases over a wide range of temperatures.

The indicated temperature value represents the mean density of the gas throughout the measured path length if pressure is constant. Only in the case of constant temperature can the indicated value be equal to the actual gas temperature.

The sensitivity of the indicated temperature measurement depends mainly on the accuracy of the knowledge of the gas constituents, on the length of time available for the measurement, and on the mechanical precision and constancy of the construction of the instrument.

Because the gas constituents change with temperature at temperatures above which dissociation occurs, dissociation correction factors have been calculated for stoichiometric mixtures of hydrocarbons and air as a function of temperature. Dissociation of the saturated hydrocarbon combustion products is negligible up to about 1800° K; the dissociation correction factor is about 1 percent at 2000° K and becomes about 3 percent at 2400° K. Above 2000° K, correction for dissociation by successive approximation is suggested.

A counting error of 3 percent, which corresponds to about 1000 total counts and therefore is readily available in most applications, can, in a properly designed instrument, give a relative error in indicated temperature measurement of about $0.006\ T/T_a$, where T is gas temperature and T_a is room (air) temperature.

The indicated temperature value is readily converted into a desired mean temperature if the shape of the temperature profile is known and the pressure is constant over the measured path.

In most cases, aluminum foil windows give a higher measuring accuracy than pinhole arrangements because they permit the passage of an X-ray beam of larger cross-sectional area. For temperatures above about 2000° K, however, pinhole arrangements have the advantage of permitting higher counting accuracy.

Experimental X-ray intensity data measured over a temperature range of 1400° to 1700° K, when compared with the burner center temperatures as determined with a thermocouple, substantiate the theoretical equations and emphasize the importance of knowledge of the temperature profiles when calculating center or mean temperatures from X-ray absorption data.

Lewis Flight Propulsion Laboratory
National Advisory Committee for Aeronautics
Cleveland, Ohio, August 20, 1951

APPENDIX A

SYMBOLS

The following symbols are used in this report:

A	X-ray beam area at distance d
B	mass-absorption coefficient
B_a	mass-absorption coefficient of air
C	absorption factor - indicative of the absorption before entering and after leaving the region of variable density
D	outside profile length
d	distance from X-ray source to detector
F	correction factor, $\frac{MB}{M_aB_a}$
F_u	correction factor, $\frac{MB}{M_aB_a}$ for undissociated gas
I	X-ray intensity after absorption
I_a	X-ray intensity at room temperature and pressure, room-temperature air reference
I_o	initial X-ray intensity
I_v	X-ray intensity, vacuum reference
K	constant, $\frac{I_oCA}{4\pi d^2}$
k	atomic emission coefficient
L	path length through gas mixture, $L = 2R$
M	molecular weight
M_a	molecular weight of air
m	molecular percentage
N	total measuring counts

N_B	total background counts
N_c	counts per minute
n	inside profile exponent
P	gas pressure
p	atomic percentage
q	outside profile exponent
R	burner radius
R_g	universal gas constant
r	radial distance
T	absolute temperature
Tr	temperature along the radial distance
T_a	room (air) temperature
T_c	absolute center temperature
$T_{D/2}$	temperature at center of outside profile
T_w	wall temperature
α	$\frac{T_c - T_w}{T_w}$
β	$\frac{T_w - T_a}{T_a}$
κ	total number of readings at a given temperature
ρ	gas density
ρ_a	air density at room temperature and pressure

APPENDIX B

EVALUATION OF THEORETICAL INTENSITIES AND ERRORS

From equation (9a) the equation for the intensity ratios may be written as:

$$\left(\frac{I}{I_a}\right)_{calc} = \exp\left\{2B_a\rho_a R\left[1 + \frac{D}{R} - Fu\,\frac{T_a}{T_c}\left(1 + \frac{\alpha}{n+1}\right) - \frac{T_a}{T_w}\,\frac{D}{R}\left(\frac{\beta}{q+1} + 1\right)\right]\right\}$$

Inserting the values

$$2^q = \frac{\frac{T_w}{T_a} - 1}{\frac{T_w}{T_{D/2}} - 1}$$

$$\beta = \frac{T_w}{T_a} - 1$$

$$\alpha = \frac{T_c}{T_w} - 1$$

$$F_u = 0.93$$

$$n = 6.0$$

$$\frac{D}{R} = 0.470$$

$$2B_a\rho_a R = 1.107$$

results in the following equation:

$$\left(\frac{I}{I_a}\right)_{calc} = \exp\left\{1.107\left[1 + 0.470\left(\frac{q}{q+1}\right) - 0.796\,\frac{T_a}{T_c} - \left[0.133 + 0.0470\left(\frac{q}{q+1}\right)\right]\frac{T_a}{T_w}\right]\right\}$$

For T_w and q related to T_c by the linear equations

$$T_w = 1.75\ T_c - 5.40\ T_a$$

and

$$q = 1.44\ \frac{T_c}{T_a} - 6.04$$

the values for $(I/I_a)_{calc}$ are given in table II.

The mean deviation of the experimental intensity ratios is given by

$$\left(\frac{\Delta I}{I}\right)_{expt} = \sqrt{\sum_{i=1}^{\kappa} \frac{\left[1 - \left(\frac{N}{\bar{N}}\right)_i\right]^2}{\kappa - 1}} \approx 0.06$$

where κ is the total number of readings at a given temperature.

The mean relative intensity error $\Delta I/I$ is given by

$$\frac{\Delta I}{I} = \frac{\sqrt{N + N_B}}{N - N_B} \approx 0.02$$

The relative temperature error $\Delta T_c/T_c$ is given by

$$\frac{\Delta T_c}{T_c} \approx \frac{\left(\frac{1}{2B_a\rho_a RF}\right)\left(\frac{n+1}{n}\right)\left(\frac{T_c}{T_a}\right)}{1 + Q}\ \frac{\Delta I}{I}$$

where

$$Q = \left(\frac{T_c}{T_a}\right)^2\left(\frac{n+1}{nF}\right)\left\{\left(\frac{D}{R}\right)\left(1 - \frac{T_a}{T_w}\right)\frac{1.44}{(q+1)^2} + 1.75\left(\frac{T_a}{T_w}\right)^2\left[\left(\frac{q}{q+1}\right)\frac{D}{R} + \frac{F}{n+1}\right]\right\}$$

REFERENCES

1. Engel, Alfred v., und Steenbeck, Max: Über die Temperatur in der Gassäule eines Lichtbogens. Wissenschaftliche Veröffentlichungen aus den Siemens-Schuckertwerken, A.-G., Heft 10, 1931, S. 155-171.

2. Fehling, H. R., and Leser, T.: Determination of the True Composition of the Products of the Theoretical Combustion with Oxygen and Oxygen-Nitrogen Mixtures at Temperatures up to 2500° C. at Atmospheric Pressure. Third Symposium on Combustion and Flame and Explosion Phenomena, The Williams & Wilkins Co. (Baltimore), 1949, pp. 634-640.

3. Huff, Vearl N., and Calvert, Clyde S.: Charts for the Computation of Equilibrium Composition of Chemical Reactions in the Carbon-Hydrogen-Oxygen-Nitrogen System at Temperatures from 2000° to 5000° K. NACA TN 1653, 1948.

4. Weltmann, Ruth N., Fairweather, Steven, and Papke, Daryl: Application of X-Ray Absorption to Measurement of Small Air-Density Gradients. NACA TN 2046, 1951.

5. Fishenden, M., and Saunders, O. A.: The Errors in Gas Temperature Measurement and Their Calculation. Jour. Inst. Fuel, vol. XII, no. 64, March 1939, pp. 5-14.

TABLE I - ATOMIC EMISSION COEFFICIENTS

Atom	k
Hydrogen	0.0002
Carbon	.20
Nitrogen	.34
Oxygen	.62
Sulfur	10.9
Chlorine	14.7
Argon	22.4

TABLE II - MEASURED AND CALCULATED VALUES OF TEMPERATURES AND INTENSITY RATIOS IN EXPERIMENTAL SETUP

Measured		Radiation corrected									
T_w (°K)	T_c (°K)	T_c (°K)	$\frac{T_w}{T_D/2}$	q_{expt}	$(I/I_a)_{expt}$	$(I/I_a)_{calc}$	$\frac{(I/I_a)_{expt}}{(I/I_a)_{calc}}$	$\left(\frac{\Delta I}{I}\right)_{expt}$	$T_{c_{calc}}$ (°K)	$\frac{T_{expt}}{T_{calc}}$	Portholes
810	1350	1387	2.10	0.62	2.60	2.69	0.96	0.0493	1360	1.02	Upper
860	1390	1429	2.02	.87	2.54	2.79	.91	.0654	1340	1.06	
930	1400	1435	2.13	.89	2.79	2.80	.99	.0890	1430	1.00	
850	1440	1484	1.96	.93	2.89	2.92	.99	.0928	1472	1.00	
1040	1460	1497	2.10	1.16							
765	1450	1501	2.14	.44							
1050	1470	1508	2.13	1.14	3.24	2.99	1.08	.0747	1655	.91	
1040	1480	1520	2.02	1.26	2.89	3.00	.96	.0527	1472	1.03	
1140	1490	1524									
1080	1500	1540	2.47	.82	3.06	3.04	1.00	.0367	1550	.99	
960	1560	1614	2.48	.57	3.08	3.18	.96	.0251	1520	1.06	
790	1570	1634	2.21	0.65	3.17	3.21	0.98	0.0175	1610	1.01	Lower
530	1590	1659			3.30	3.25	1.01		1690	.98	
935	1620	1679	2.15	.88	3.21	3.27	.98	.0574	1630	1.03	
975	1640	1705	1.97	1.21							

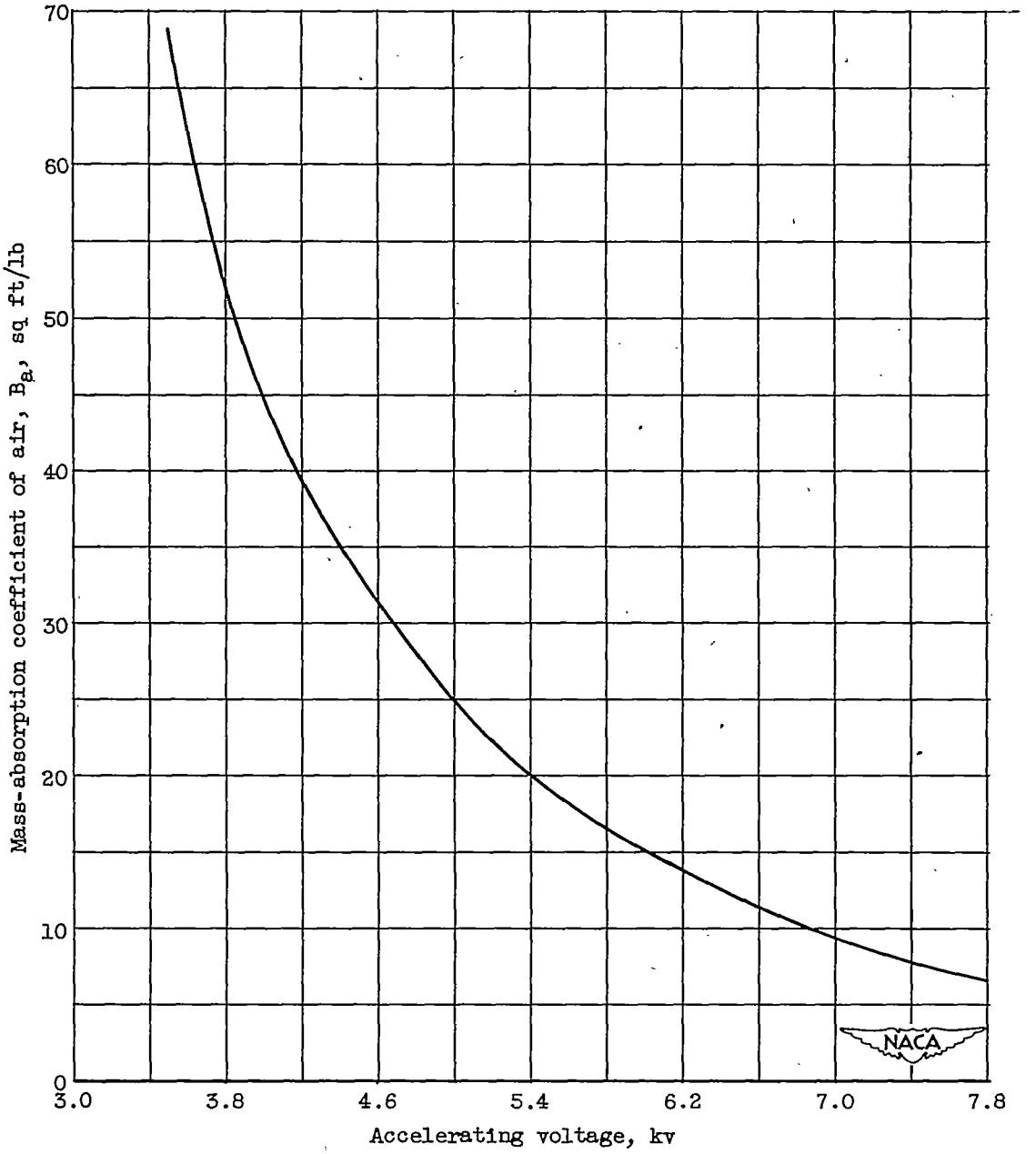

Figure 1. - Variation of mass-absorption coefficient of air with accelerating voltage applied to X-ray tube.

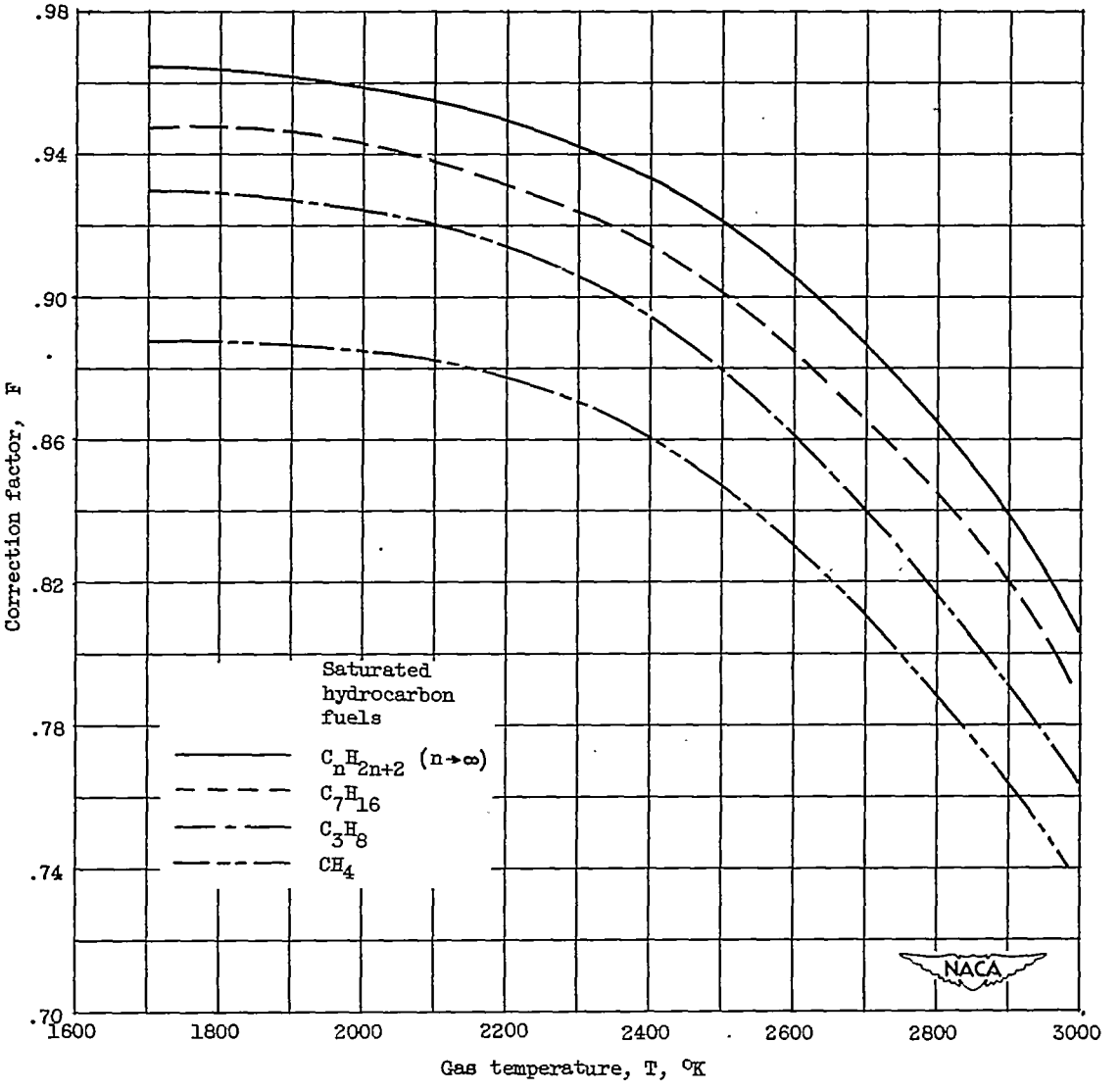

Figure 2. - Variation of correction factor F with temperature for products of stoichiometric combustion of saturated hydrocarbons with air.

2401

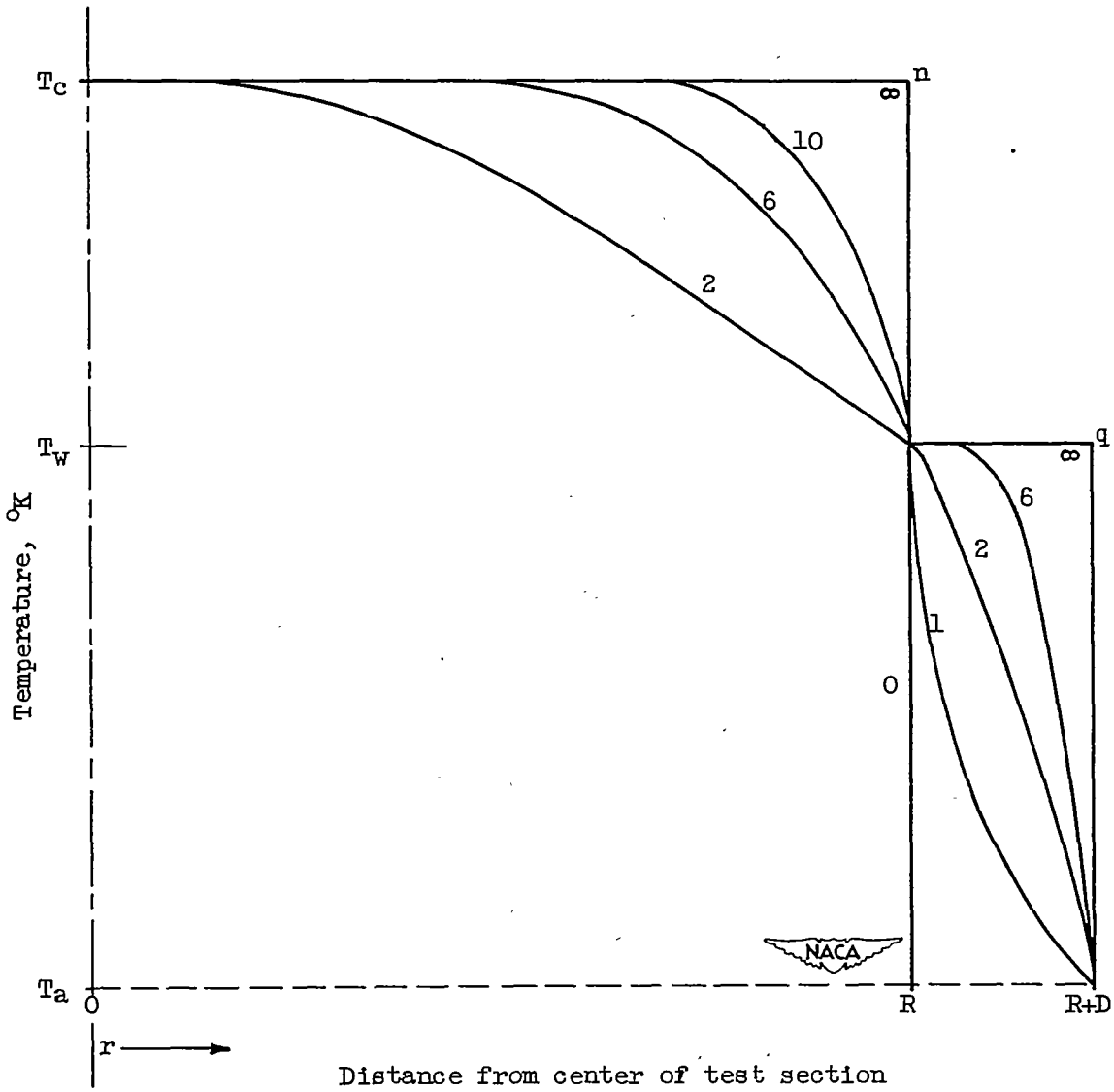

Figure 3. - Representative temperature profiles inside and outside of test section.

$$T_r = \frac{T_c}{1+\alpha\left(\frac{r}{R}\right)^n} \text{ for } r < R, \qquad \alpha = \frac{T_c}{T_w} - 1 = \frac{1}{2};$$

$$T_r = \frac{T_w}{1+\beta\left(\frac{r}{R}\right)^q} \text{ for } R < r < R+D, \quad \beta = \frac{T_w}{T_a} - 1 = 3.$$

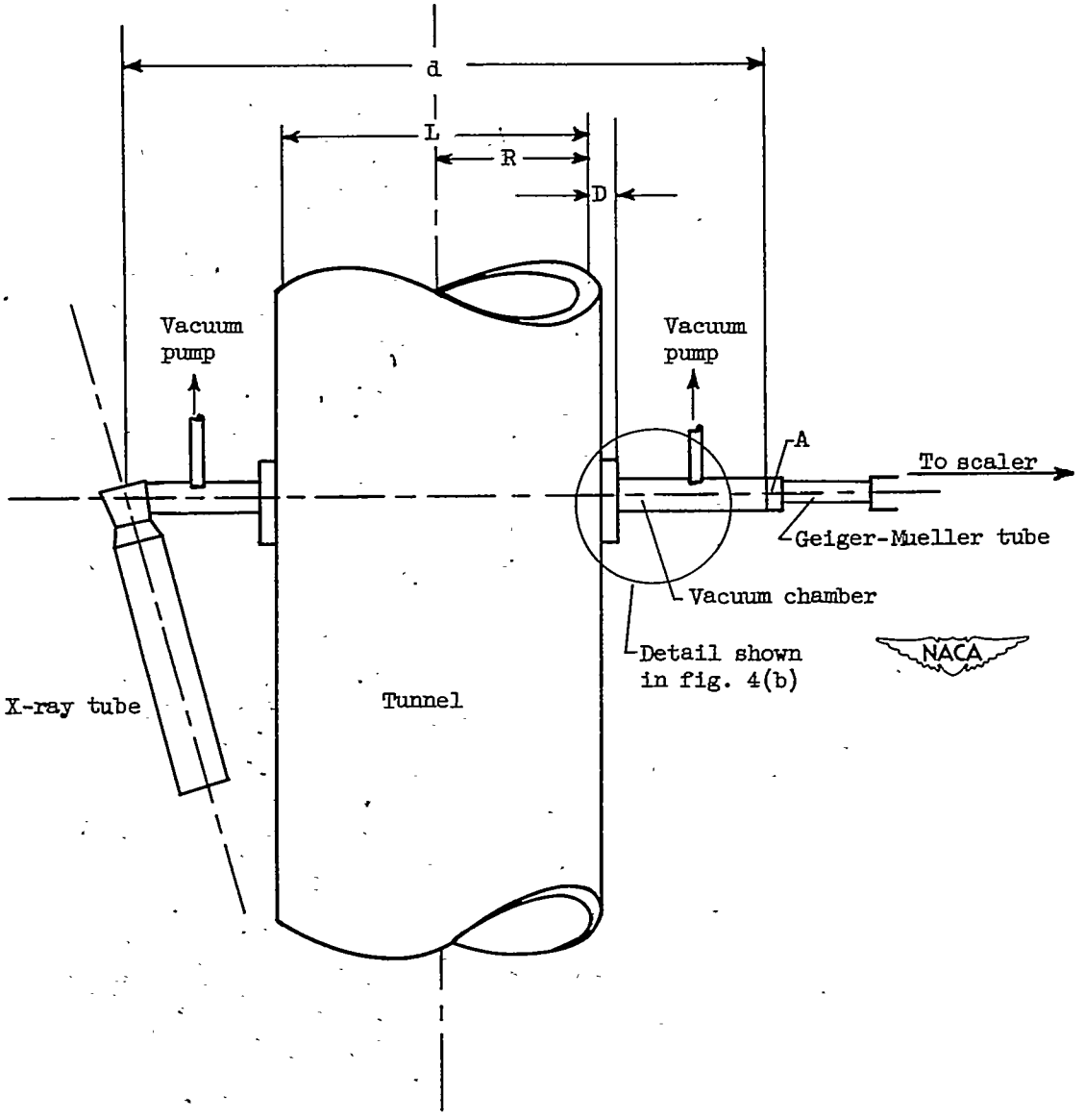

(a) Over-all arrangement of apparatus.

Figure 4. - Schematic diagram of X-ray absorption instrument.

2401

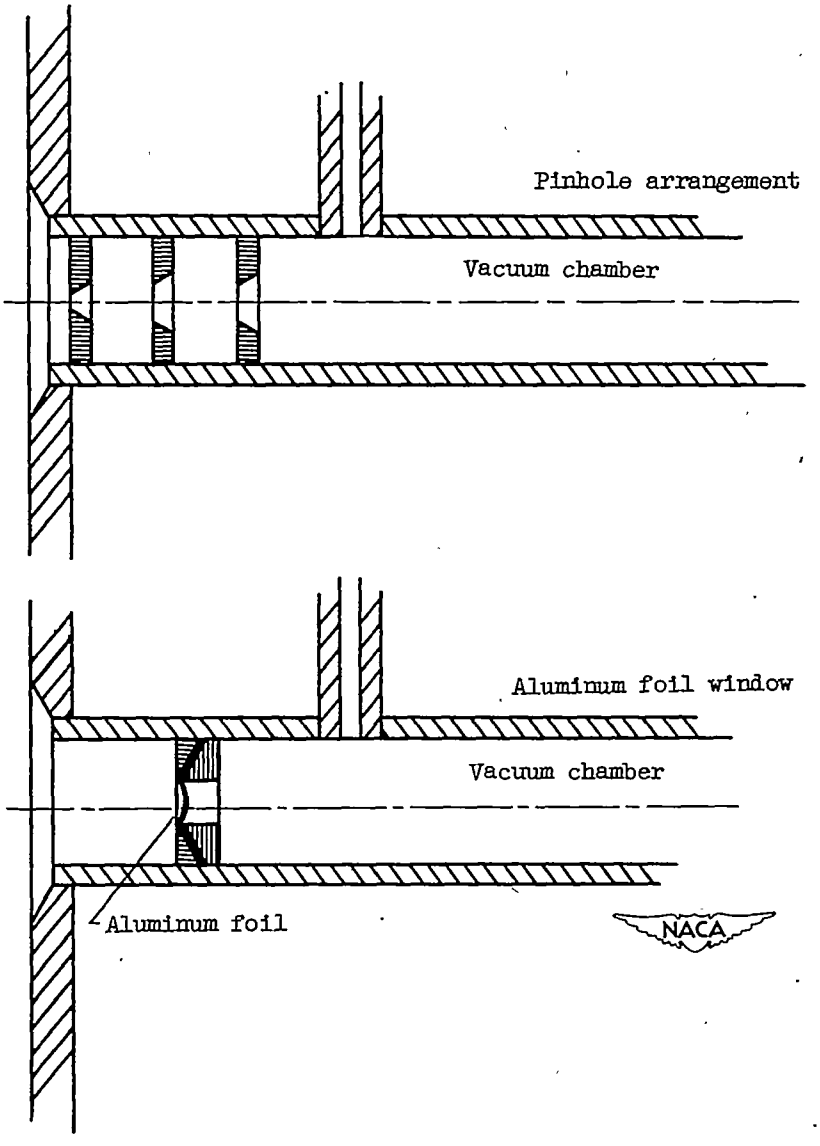

(b) Aluminum foil window and pinhole arrangement.

Figure 4. - Concluded. Schematic diagram of X-ray absorption instrument.

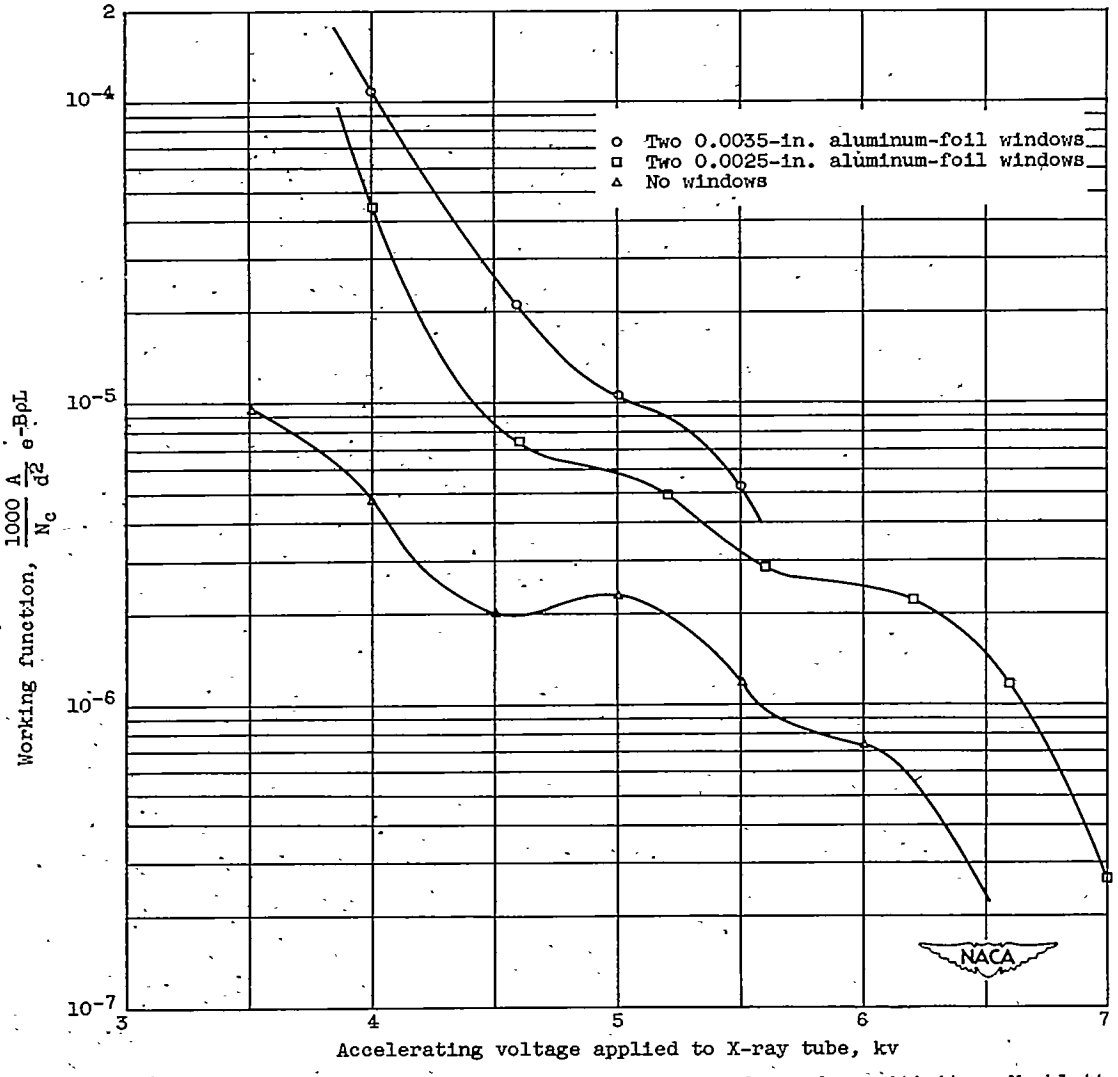

Figure 5. - Working curves for calculation of voltages and sensitivity. Machlett, Type A-2 Diffraction Tube, with a tungsten target at 15-milliampere filament current.

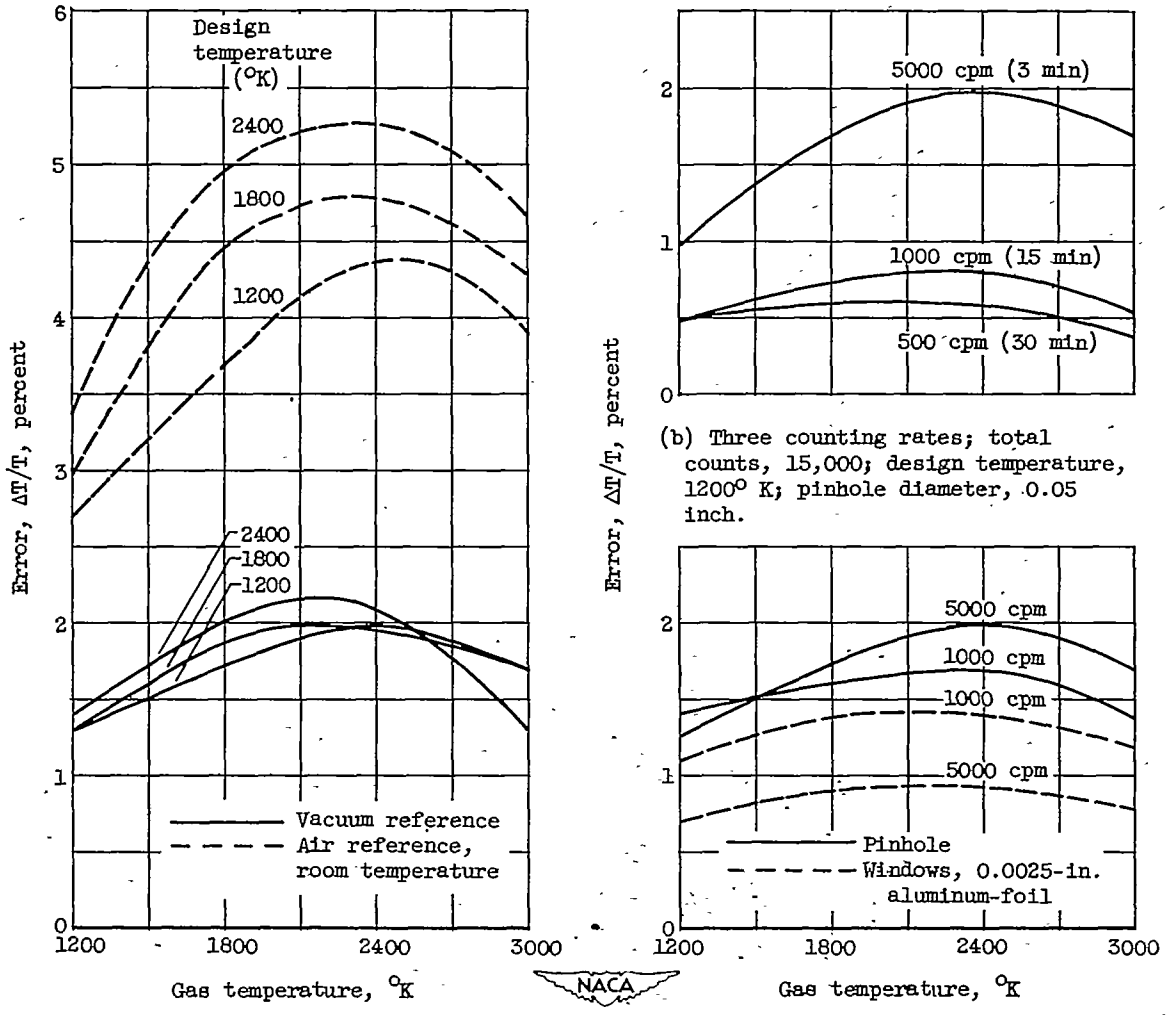

(a) Counting rate, 5000 counts per minute; counting period, 3 minutes; three design temperatures; vacuum and air references; pinhole diameter, 0.05 inch.

(b) Three counting rates; total counts, 15,000; design temperature, 1200° K; pinhole diameter, 0.05 inch.

(c) Two counting rates; counting time, 3 minutes; design temperature, 1200° K; pinhole diameter, 0.05 inch; window diameter, 0.20 inch.

Figure 6. - Variation of calculated errors with temperature for 1.5-foot path length hot tunnel using stoichiometric saturated hydrocarbon fuel mixtures.

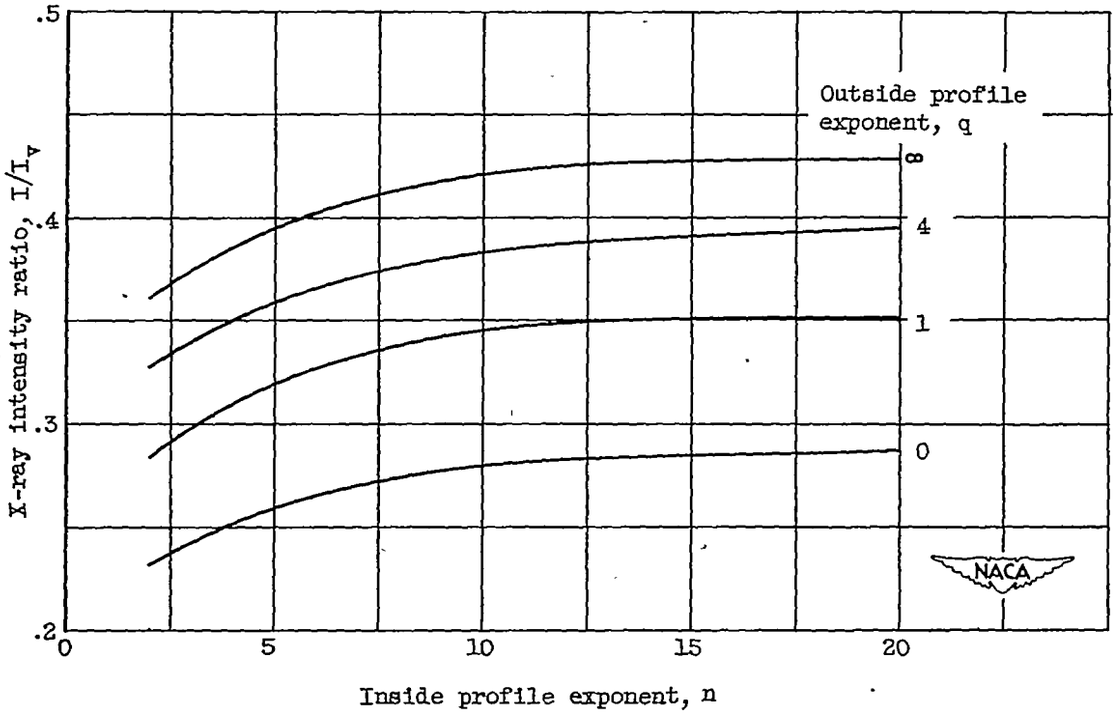

Figure 7. - Variation of X-ray intensity ratio with inside profile exponent for various outside profile exponents. Center gas temperature, 1800° K; wall temperature, 900° K; room (air) temperature, 300° K; window diameter, 0.20 inch at distance of 2 feet; acceleration voltage, 4.15 kilovolts; combustion of saturated hydrocarbons.

2401

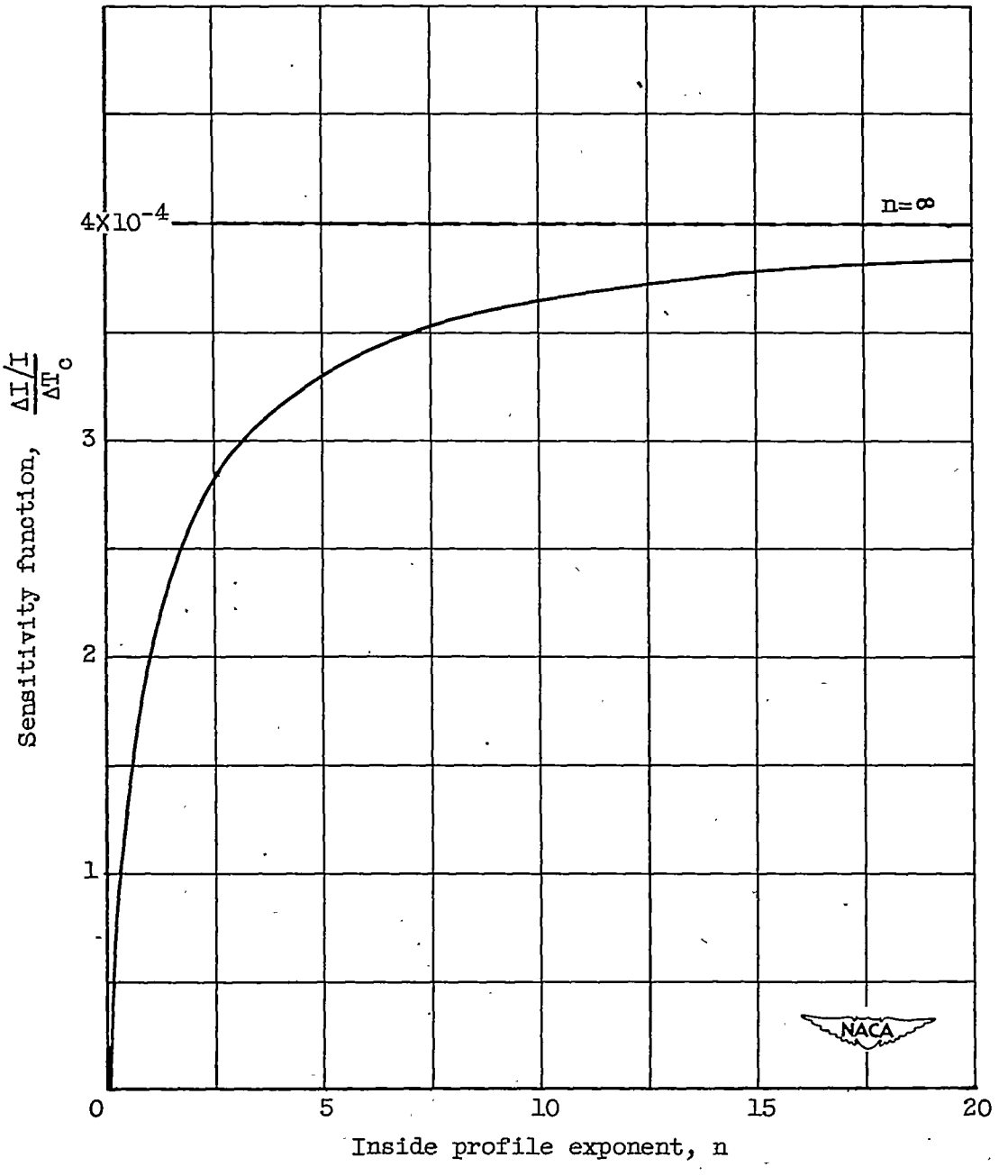

Figure 8. - Variation of sensitivity function with inside profile exponent. Center temperature, 1800° K; wall temperature, 900° K; room (air) temperature, 300° K; window diameter, 0.20 inch at distance of 2 feet; acceleration voltage, 4.15 kilovolts; combustion of saturated hydrocarbons.

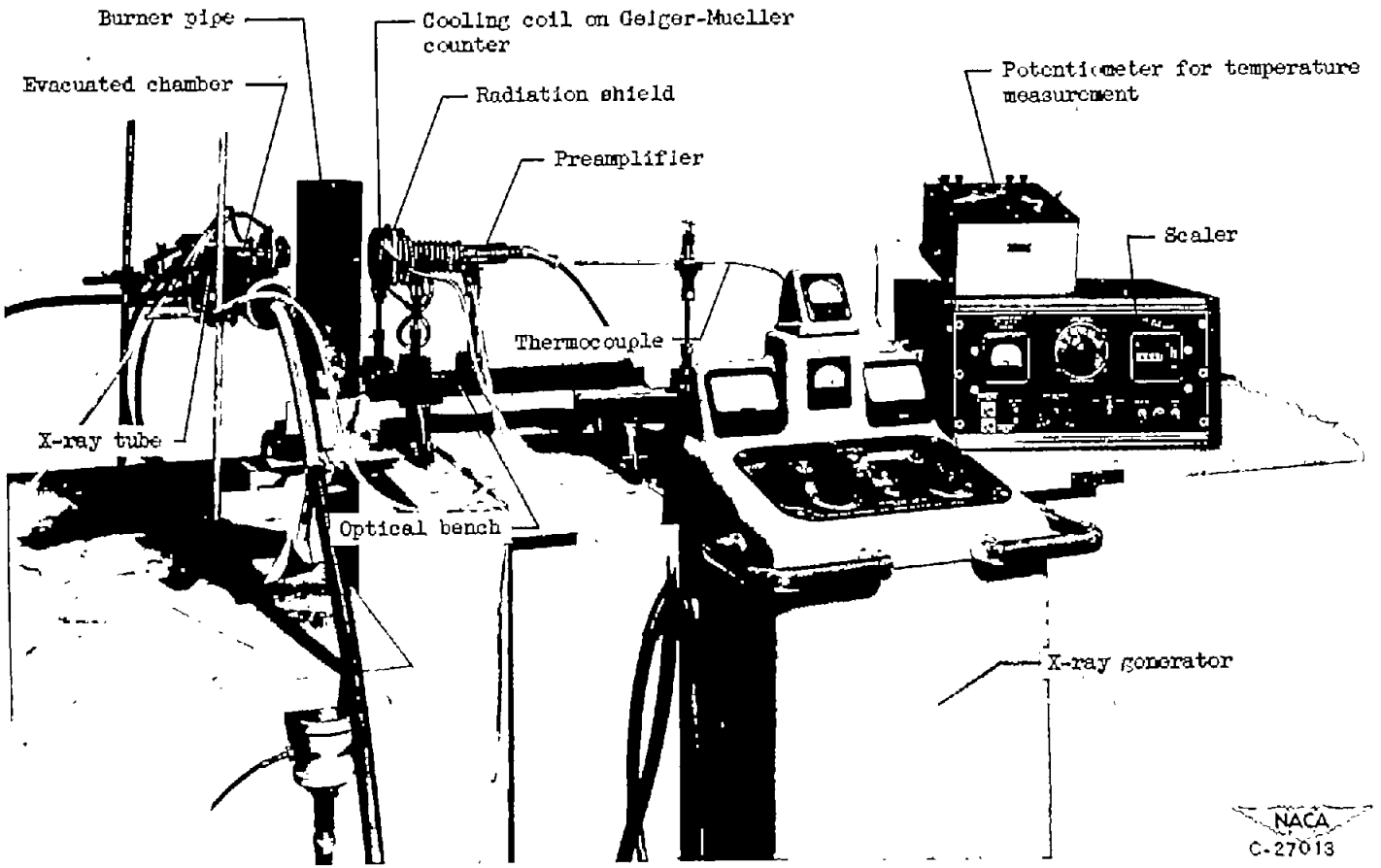

(a) View of gas burner pipe, X-ray equipment and associated parts.

Figure 9. - Experimental setup.

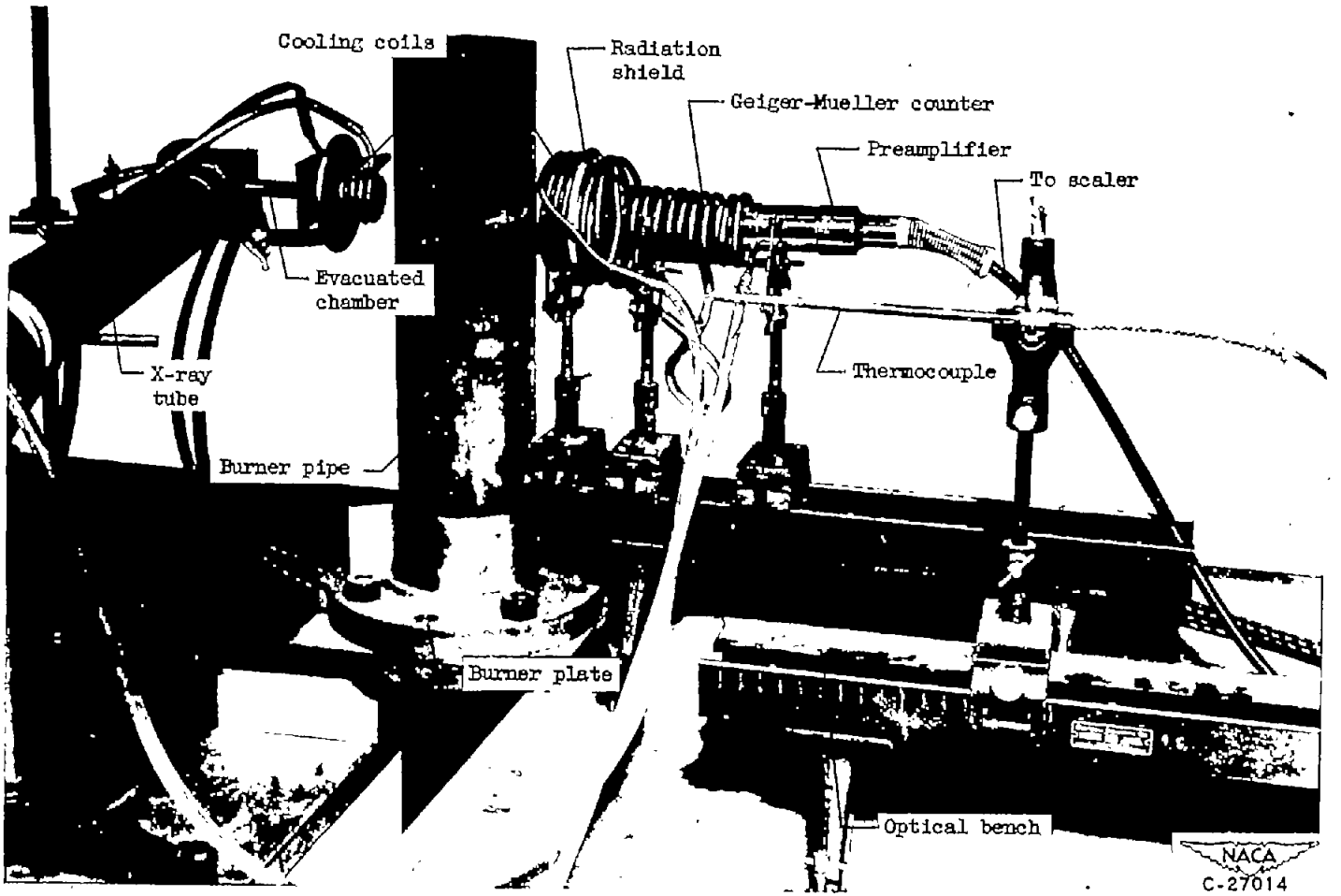

(b) Enlarged view of gas burner pipe and associated parts.

Figure 9. - Concluded. Experimental setup.

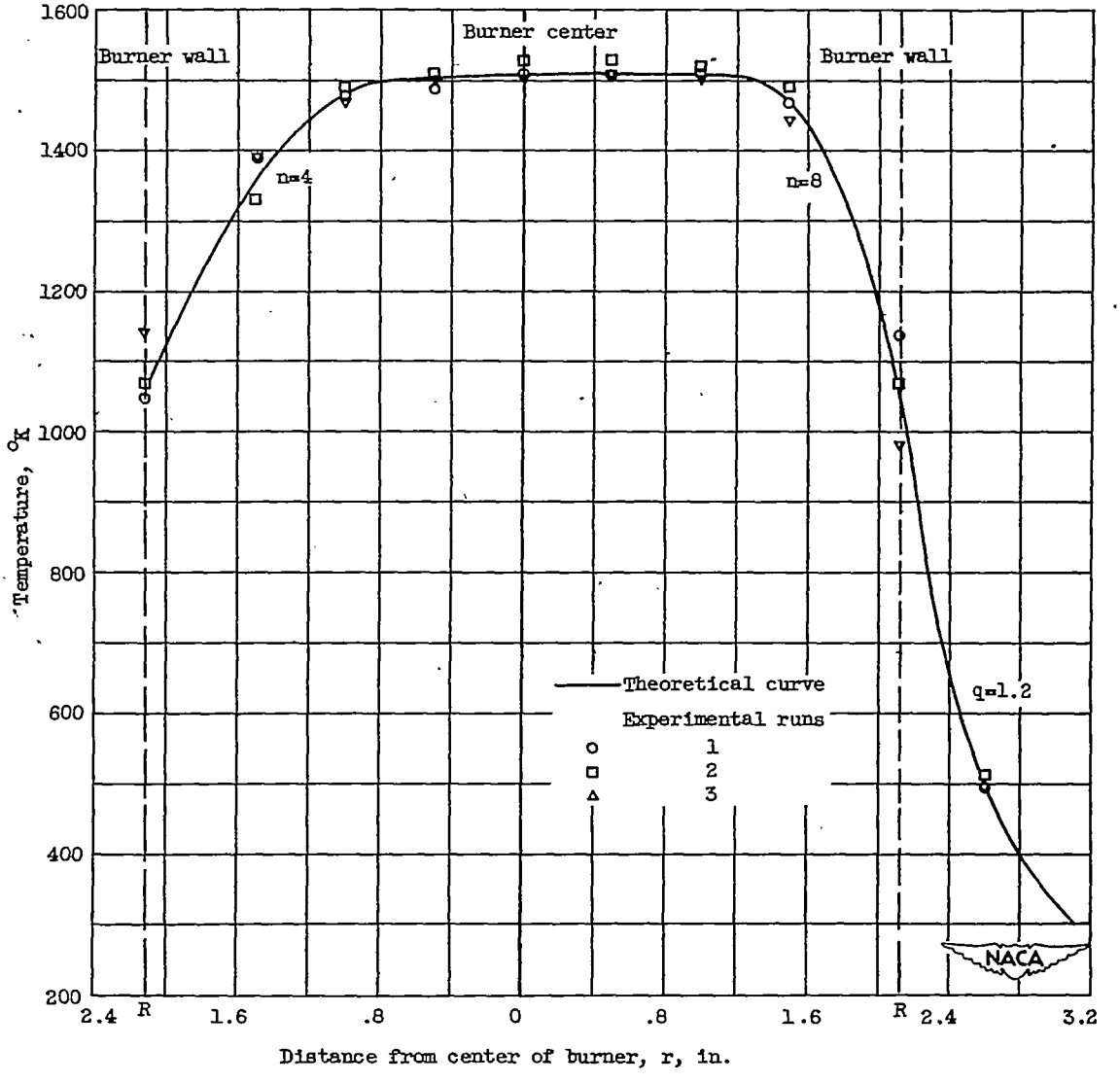

Figure 10. - Inside and outside tempeirature profiles. Theoretical-curve parameters: Center temperature, 1510° K; wall temperature, 1050° K; temperature at center of outside profile, 500° K.

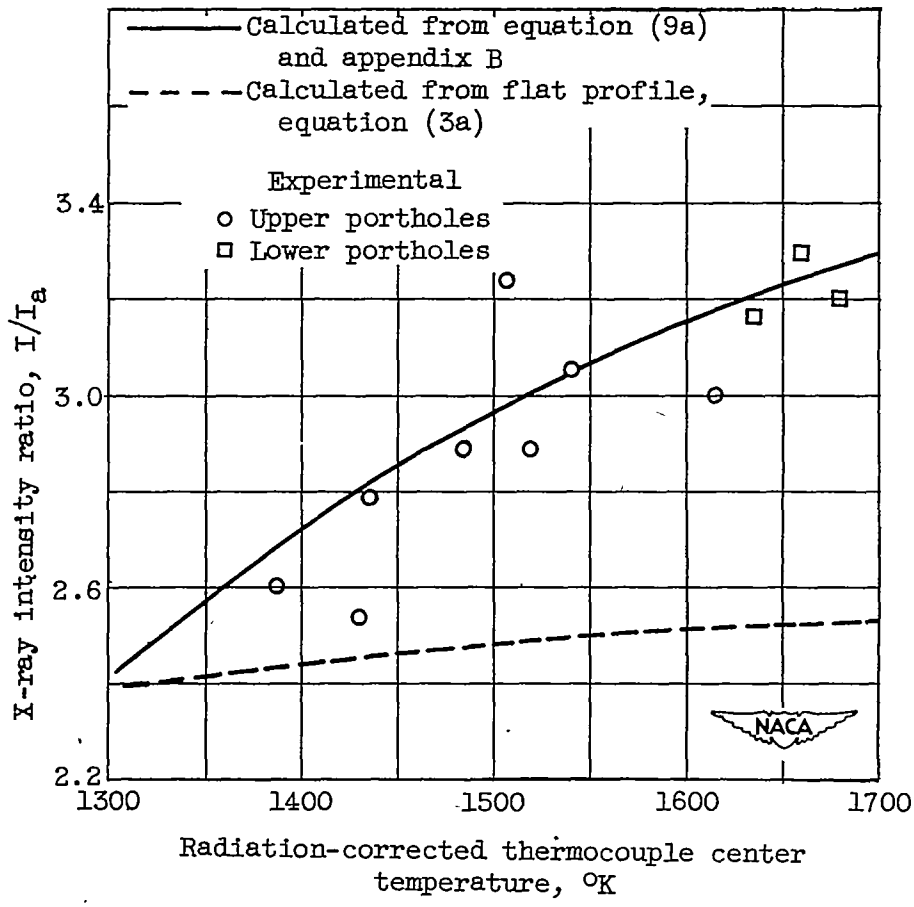

Figure 11. - Experimental and theoretical values of X-ray intensity ratios as a function of radiation-corrected thermocouple center temperatures.

NACA-Langley - 12-14-51 - 100